



HAL
open science

Synergistic mineralization of ofloxacin in electro-Fenton process with BDD anode: Reactivity and mechanism

Weilu Yang, Nihal Oturan, Jialin Liang, Mehmet Oturan

► To cite this version:

Weilu Yang, Nihal Oturan, Jialin Liang, Mehmet Oturan. Synergistic mineralization of ofloxacin in electro-Fenton process with BDD anode: Reactivity and mechanism. *Separation and Purification Technology*, 2023, 319, pp.124039. 10.1016/j.seppur.2023.124039 . hal-04126207

HAL Id: hal-04126207

<https://hal.science/hal-04126207>

Submitted on 13 Jun 2023

HAL is a multi-disciplinary open access archive for the deposit and dissemination of scientific research documents, whether they are published or not. The documents may come from teaching and research institutions in France or abroad, or from public or private research centers.

L'archive ouverte pluridisciplinaire **HAL**, est destinée au dépôt et à la diffusion de documents scientifiques de niveau recherche, publiés ou non, émanant des établissements d'enseignement et de recherche français ou étrangers, des laboratoires publics ou privés.

Synergistic mineralization of ofloxacin in electro-Fenton process with BDD anode: Reactivity and mechanism

Weilu Yang^{a,b}, Nihal Oturan^c, Jialin Liang^a, Mehmet A. Oturan^{c, *}

^a *College of Resources and Environment, Zhongkai University of Agriculture and Engineering, Guangzhou 510225, China*

^b *Guangdong Key Laboratory of Environmental Pollution and Health, School of Environment, Jinan University, Guangzhou 511443, China*

^c *Université Gustave Eiffel, Laboratoire Géomatériaux et Environnement, EA 4508, UPEM, 5 Bd Descartes, 77454 Marne-la-Vallée, Cedex 2, France.*

* Corresponding author:

Mehmet.oturan@univ-eiffel.fr (Mehmet A. Oturan)

1 Abstract

2 This study aimed at exploring the performance of the electro-Fenton (EF) process with a boron-
3 doped diamond (BDD) anode and an electrochemically exfoliated graphene-based cathode
4 (EEGr), for removal of antibiotic ofloxacin (OFLO) from contaminated water. Compared with
5 anodic oxidation (AO) process with BDD anode, the EF process with BDD anode (EF-BDD)
6 could improve the decay kinetics of OFLO by 1.4–2.6 times and reduce the disposal cost by
7 28%–41%. Removal efficiency of TOC in EF-BDD process under 4.2 mA cm^{-2} was better than
8 in AO process under 8.3 mA cm^{-2} , pointing out that the cost effectiveness of the EF process for
9 mineralization of OFLO under low current density conditions. This advantage is due to the
10 simultaneous formation of homogeneous ($\cdot\text{OH}$) and heterogeneous ($\text{BDD}(\cdot\text{OH})$) hydroxyl
11 radicals in the process. The synergistic factor of $\cdot\text{OH}$ and $\text{BDD}(\cdot\text{OH})$ for mineralization of
12 OFLO decreased with the current density rising from $4.2 (0.28)$ to $16.6 \text{ mA cm}^{-2} (-0.08)$. Decay
13 kinetics of OFLO in the EF-BDD and AO were more converging under higher current densities
14 owing to the production of large amount of $\text{BDD}(\cdot\text{OH})$. In the EF-BDD, a trade-off should be
15 considered between accumulated $\text{BDD}(\cdot\text{OH})$ on the surface of BDD anode and H_2O_2
16 generation on the cathode. Absolute rate constant for oxidation of OFLO by $\cdot\text{OH}$ (k_{OFLO}) was
17 calculated to be $3.86 \times 10^9 \text{ M}^{-1} \text{ s}^{-1}$. Evolution of carboxylic acids and inorganic ions as well as
18 toxicity assessment were followed during the treatment of OFLO solutions. Results obtained
19 proved that the EF-BDD process is outstanding for oxidative degradation of OFLO thanks to
20 the synergistic effect of $\cdot\text{OH}$ and $\text{BDD}(\cdot\text{OH})$. These very strong oxidants being non-selective,
21 this result can be extended to the treatment of antibiotic organic pollutants.

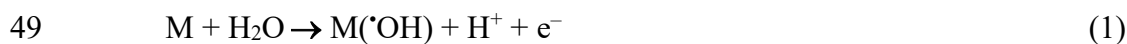
22

23 **Keywords:** Electro-Fenton, Anodic oxidation; BDD anode, Synergistic catalysis, Hydroxyl
24 radial, Pharmaceutical wastewater

25

26 1. Introduction

27 Antibiotics are largely used throughout the world. The majority of discharged antibiotics and
28 their metabolites escape from being eliminated in the traditional wastewater treatment plants
29 due to slight solubility and strong resistance to degradation by conventional biological or
30 chemical processes [1,2]. Types of antibiotics and their incomplete transformation products
31 were detected in multiple aquatic ecosystems and have drawn close attention from researchers
32 and public authorities [3]. These pollutants pass through the municipal water treatment plants,
33 since they are not designed to retain this kind of pollutants. Removal of these pollutants from
34 aquatic environments, as eco-toxicological threats to humans and aquatic animals, has been a
35 great challenge. In contrast to the conventional treatment processes, the electrochemical
36 advanced oxidation processes (EAOPs) have attracted great interest for removing efficiently
37 persistent/toxic organic pollutants from water via in situ generated oxidant free radicals [4-7].
38 As one of the most popular EAOPs, the electro-Fenton (EF) process have gained prominence
39 owing to its economic feasibility and remarkable mineralization efficiency [8,9]. This
40 promising technology has been successfully applied for complete mineralization of various
41 refractory organic pollutants including pharmaceutical compounds [10-13]. In the EF process,
42 homogeneous $\cdot\text{OH}$ radicals ($E_{\text{OH}/\text{H}_2\text{O}}^0 = 2.8 \text{ V/SHE}$) are generated electrocatalytically in the
43 bulk solution through Fenton's reaction [4,5,7,16]. On the other side, the anodic oxidation (AO)
44 process provides heterogeneous $\cdot\text{OH}$ radicals on the surface of anodes with high O_2 evolution
45 overvoltage [17,18]. The AO processes belong to direct electrooxidation and usually involves
46 the mass transfer limitation [19,20]. The use of an appropriate anode (M) can produce
47 heterogeneous radicals ($\text{M}(\cdot\text{OH})$) via oxidation of water on the surface of anode (Eq. (1))
48 [21,22].



50 The contribution of $M(\cdot\text{OH})$ to EF process is strongly related to the nature of anode material,
51 as well as in the overall performance of AO [23]. Anodes characterized with high O_2 -evolution
52 overpotential are regarded as “non-active” anodes, while those with low O_2 -evolution
53 overpotential are of the “active anodes” type. In the first case, $M(\text{OH})$ are barely adsorbed on
54 the surface (physisorption) while in the second case they are strongly adsorbed
55 (chemisorption). Boron-doped diamond (BDD), as typical “non-active” anode, is the most
56 potent anode for AO due to its high O_2 evolution overpotential (around 2.2 V/SHE), high
57 stability and available of physisorbed BDD($\cdot\text{OH}$) [24,25]. In contrast to the chemisorbed
58 $M(\cdot\text{OH})$ on the surface of active anodes such as Pt and DSA anodes, a large amount of
59 physically adsorbed BDD($\cdot\text{OH}$) enhance the effectiveness of the EF process, especially for the
60 complete destruction of aliphatics [26]. In EF processes with BDD anode (EF-BDD process),
61 the oxidative degradation of organics can be regarded as a synergistic effect of heterogeneous
62 BDD($\cdot\text{OH}$) (formed at the surface of BDD anode) and homogeneous $\cdot\text{OH}$ generated in solution
63 [27, 28]. We previously showed that BDD anode provides outstanding performances for
64 mineralization of drug imatinib solution compared to other three anodes (DSA, Pt and Ti_4O_7),
65 with complete mineralization of imatinib solution (corresponding to 24.11 mg L^{-1} initial TOC)
66 in EF-BDD process under 12.5 mA cm^{-2} [19].

67 This study focuses on the contribution of BDD($\cdot\text{OH}$) in the EF-BDD process, at different stage
68 and under different operating conditions during the treatment of pharmaceutical wastewater.
69 Indeed, there are very few studies devoted to this topic [25] and further research is needed to
70 clarify the synergistic effect of BDD($\cdot\text{OH}$) on the EF-BDD process during wastewater
71 treatment. Therefore, the oxidative degradation and mineralization of a synthetic solution of a
72 fluoroquinolone antibiotic, the ofloxacin, largely used for the treatment of a number of bacterial
73 infections, was studied by electro-Fenton process with BDD anode. The primary aims of the
74 study were (i) identify the outstanding performance of BDD-EF for removal of OFLO, (ii)

75 evaluate relative contributions of homogeneous $\cdot\text{OH}$ and heterogeneous BDD($\cdot\text{OH}$) during
76 oxidation of OFLO by EF-BDD process, (iii) explore the synergistic effect of homogeneous
77 $\cdot\text{OH}$ and heterogeneous BDD($\cdot\text{OH}$) hydroxyl radicals for mineralization of OFLO in EF-BDD
78 process, (iv) elucidate the possible pathway of OFLO degradation and (v) assess acute toxicity
79 (LC50), developmental toxicity, bioaccumulation factor and mutagenicity by quantitative
80 structure-activity relationship using the Toxicity Estimation Software Tool.

81

82 **2. Materials and methods**

83 *2.1. Chemicals and reagents*

84 Carbon felt (CF) and graphite foil were purchased from Beijing Jinglong Special Carbon
85 (Beijing, China), polytetrafluoroethylene was obtained from Shanghai Hesun Electric
86 (Shanghai, China). Methanol, ethanol, sulfuric acid, potassium hydroxide, anhydrous sodium
87 sulfate (Na_2SO_4 ; 99–100% purity), H_2O_2 (30% by weight) and iron (II) sulphate heptahydrate
88 (99.5%) were purchased from Tianjin Kemiou Chemical Reagent (Tianjin, China). Analytical
89 grade OFLO ($\text{C}_{18}\text{H}_{20}\text{FN}_3\text{O}_4$, MW: 361.1 g mol^{-1} , CAS n^o: 82419-36-1, 99.9% purity, with
90 chemical structure given in Table 2), phosphoric acid, acetonitrile, 4-hydroxybenzoic acid,
91 tertiary butyl alcohol and benzoquinone were supplied by Aladdin Chemical Reagent
92 (Shanghai, China). Dimethyl sulfoxide, potassium titanium (IV) oxalate, and 2,4-
93 dinitrophenylhydrazine were purchased from Beijing Puyihua Science and Technology
94 (Beijing, China).

95

96 *2.2 Preparation of EEGr-CF cathodes*

97 The graphene used in this study was synthesized via electrochemical exfoliation of graphite
98 foil (for simplification, it was noted as EEGr). The graphene-based cathode (EEGr-CF) was

99 prepared with EEGr, carbon black, PTFE, deionized water and ethanol as described in reference
100 [29]. A certain amount of EEGr and carbon black powder were mixed at a mass ratio of 1:4,
101 with PTFE, ethanol and deionized water forming a semifluid upon rapid shaking for 15 s. The
102 milky mixture was coated on both sides of the pre-treated CF. After drying at ambient
103 temperature; CF was placed in a tube furnace under nitrogen atmosphere and annealed at 360
104 °C for 30 min, which was marked as EEGr-CF cathode.

105

106 2.3. Degradation experiments

107 Degradation of OFLO in EF-BDD, AO and EF-DSA processes were carried out in 250 mL
108 single-chamber electrolytic cells. The effective surface area of BDD and DSA anodes was $4 \times$
109 6 cm^2 , and that of the prepared EEGr-CF cathodes was $2 \times 3 \text{ cm}^2$. These electrodes were used
110 both in EF and AO processes. The BDD anode was replaced with DSA in order to exclude the
111 heterogeneous $\cdot\text{OH}$ produced in EF-DSA, because this anode generate only a few DSA($\cdot\text{OH}$).
112 The distance between the anodes and cathodes was 2 cm. Aeration was provided to the solution
113 at a flow rate of 0.75 L min^{-1} to maintain it a O_2 -saturated level. Aqueous solution of 0.1 mM
114 OFLO containing 0.05 M Na_2SO_4 as electrolyte was adjusted to pH 3. During the degradation
115 tests, liquid samples were withdrawn periodically, filtered with $0.45 \mu\text{m}$ PTFE membrane
116 filters, and immediately mixed with methanol to scavenge the reactive species and terminate
117 the oxidation reactions. All of the experiments were operated with deionized water at ambient
118 temperature.

119

120 2.4. Analytical procedures and calculation methods

121 Concentration of OFLO was measured with a Thermo Fisher Scientific U3000 high
122 performance liquid chromatograph (MA, USA) equipped with a C18 column ($3 \text{ mm} \times 100 \text{ mm}$,
123 $3 \mu\text{m}$) and with a diode array detector. Analysis was carried out under following conditions:

124 mobile phase: HPLC-grade acetonitrile/phosphoric acid/water (15:1:84 in volume); flow rate
125 of 0.25 mL min⁻¹; column oven temperature at 30 °C and wavelength of 288 nm. OFLO
126 transformation products (OTPs) generated during the degradation process were identified with
127 an Agilent 7890 A/5975 C gas chromatograph-mass spectrometer (CA, USA) interfaced with
128 a HP-5 MS capillary column (30 m × 0.25 mm, 0.25 μm).

129 The degradation efficiency of a target pollutant was calculated by the following equation:

$$130 \quad R\% = (C_0 - C_t) / C_0 \times 100 \quad (1)$$

131 The pseudo-first-order rate constant (k_{app}) for oxidative degradation of OFLO was determined
132 by using Eq. (2):

$$133 \quad \text{Ln}(C_t / C_0) = -k \times t \quad (2)$$

134 where C_0 and C_t were concentrations of the target pollutant at the beginning of electrolysis and
135 at time t , respectively.

136 The total organic carbon (TOC) removal efficiency was calculated according to TOC decay
137 measurement as follow:

$$138 \quad \text{TOC}(\%) = (\Delta(\text{TOC})_{\text{exp}} / \text{TOC}_0) \times 100$$

139 Total organic carbon (TOC) of OFLO (0.1 mM solution corresponding to an initial TOC of
140 21.6 mg L⁻¹) was measured with an Analytik jena multi N/C 3100 TOC analyzer (Jena,
141 Germany). The concentration of H₂O₂ was measured by potassium titanium (IV) oxalate
142 method using an UV759 UV-Vis spectrophotometer (Shanghai, China). Carboxylic acids
143 generated during the mineralization of OFLO were identified with an Agilent 1260 HPLC (CA,
144 USA) equipped with a Carbomix H-NP10 column (6.0 μm, 7.8 × 300 mm) at wavelength of
145 210 nm. Mobile phase and flow rate were H₂SO₄ (0.25 mM) and 0.6 mL min⁻¹. Inorganic ions
146 generated during EF process were monitored with a Dionex ICS-900 ion chromatograph (CA,

147 USA). Ofloxacin transformation products (OTPs) were detected with HPLC and GC-MS (Text
 148 S1-1). Acute toxicity (LC50), developmental toxicity, bioaccumulation factor were evaluated
 149 by quantitative structure-activity relationship using Toxicity Estimation Software Tool.

150 The relative contributions of homogeneous $\cdot\text{OH}$ and heterogeneous BDD($\cdot\text{OH}$) for TOC
 151 removal were calculated according to the Eq. (2) and (3):

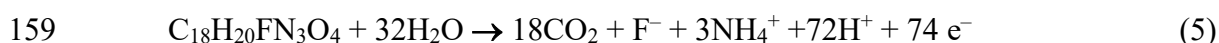
$$152 \quad R\% (\cdot\text{OH}) = 100 (TOC_{EF-BDD} - TOC_{AO}) / TOC_{EF-BDD} \quad (2)$$

$$153 \quad R\% (\text{BDD}(\cdot\text{OH})) = 100 (TOC_{AO}) / TOC_{EF-BDD} \quad (3)$$

154 where TOC_{EF-BDD} and TOC_{AO} were TOC decay values obtained in the EF-BDD and AO
 155 processes, respectively.

156 The mineralization current efficiency (MCE) and energy consumption (EC) of OFLO solution
 157 were calculated according to following equations:

$$158 \quad \text{MCE \%} = 100 n F V_s \Delta(\text{TOC})_{\text{exp}} / 4.32 \times 10^7 m I t \quad (4)$$



$$160 \quad \text{EC (kWh (gTOC)}^{-1}) = U I t / V_s \Delta(\text{TOC})_{\text{exp}} \quad (6)$$

161 where n is the number of electron (which was taken as 74 assuming that the majority of N atom
 162 contained in OFLO molecule was released as NH_4^+ in eq. (5)) consumed per mol of OFLO in
 163 the electrochemical mineralization reaction. F is the Faraday constant (96485 C mol^{-1}),
 164 $\Delta(\text{TOC})_{\text{exp}}$ means the TOC decay at t time, 4.32×10^7 represents a conversion factor to
 165 homogenize units ($3600 \text{ s h}^{-1} \times 12000 \text{ mg of C mol}^{-1}$). U , I , t are the average cell voltage (V),
 166 the current applied (A) and the electrolysis time (h), respectively.

167 Synergistic factor (SF) was calculated to confirm the synergistic effects of homogeneous $\cdot\text{OH}$
 168 and heterogeneous BDD($\cdot\text{OH}$) for oxidation of organics.

$$169 \quad \text{SF} = [k_{EF-BDD} - (k_{EF-DSA} + k_{AO})] / (k_{EF-DSA} + k_{AO}) \quad (7)$$

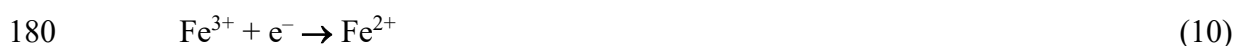
170 where k_{EF-BDD} , k_{EF-DSA} and k_{AO} were kinetic constants of OFLO oxidation in EF-BDD, EF-DSA
171 and AO processes, respectively.

172

173 3. Results and discussion

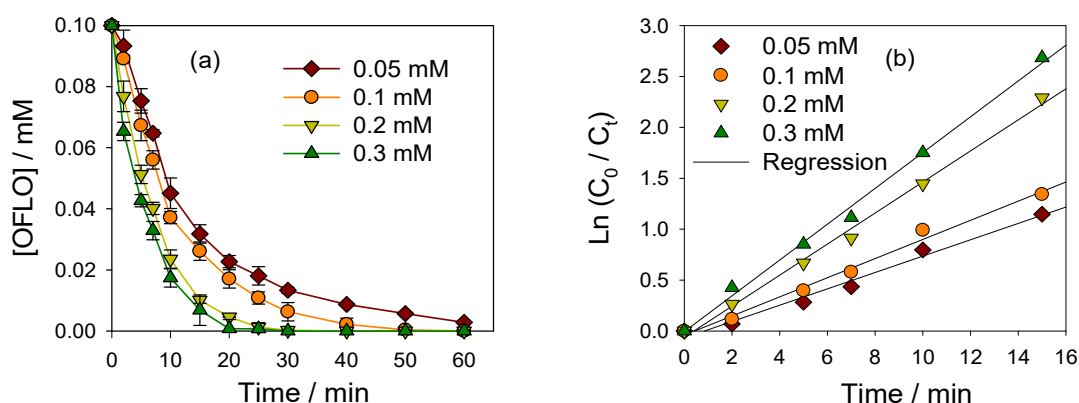
174 3.1. Comparative oxidation of OFLO by EF process

175 In EF process, degradation of organics is carried out by homogeneous $\cdot\text{OH}$ through Fenton
176 reaction (Eq. (2)) for which the Fenton's reagent ($\text{H}_2\text{O}_2 + \text{Fe}^{2+}$) is electrochemically generated
177 in the treated solution (Eqs. (8) and (9)):



181 To evaluate the comparative efficiency of different EAOPs (EF-BDD, AO and EF-DSA),
182 oxidative degradation 0.1 mM OFLO was studied under current density of 8.3 mA cm^{-2} . First,
183 preliminary experiments were performed to determine the better concentration of catalyst
184 (Fe^{2+}), since it affects the generation of homogeneous $\cdot\text{OH}$ in the solution [30, 31]. For this, the
185 solution pH was set to 3 as this value is well-known to be suitable for EF process [5, 7, 12, 16,
186 26, 35]. The complete degradation of 0.1 mM OFLO reached in 60, 50, 25 and 20 min for
187 catalyst concentration of 0.05, 0.1, 0.2 and 0.3 mM Fe^{2+} , respectively (Fig. 1). The apparent
188 rate constants (k_{app}) was 0.07 and 0.09 min^{-1} with 0.05 and 0.1 mM Fe^{2+} , and fluctuated little
189 with 0.2 (0.15 min^{-1}) and 0.3 mM (0.17 min^{-1}) Fe^{2+} for OFLO removal in EF process. However,
190 the concentration of 0.2 mM Fe^{2+} was chosen as the proper concentration of catalyst for the
191 following EF experiments. Low concentration of Fe^{2+} will guarantee the continuous reaction
192 via reduction of Fe^{3+} (Eq. (10)) generated in Fenton reaction [32,33] and avoids the wasting of
193 generated $\cdot\text{OH}$ through the reaction given in Eq. (11) which is favored at high Fe^{2+}

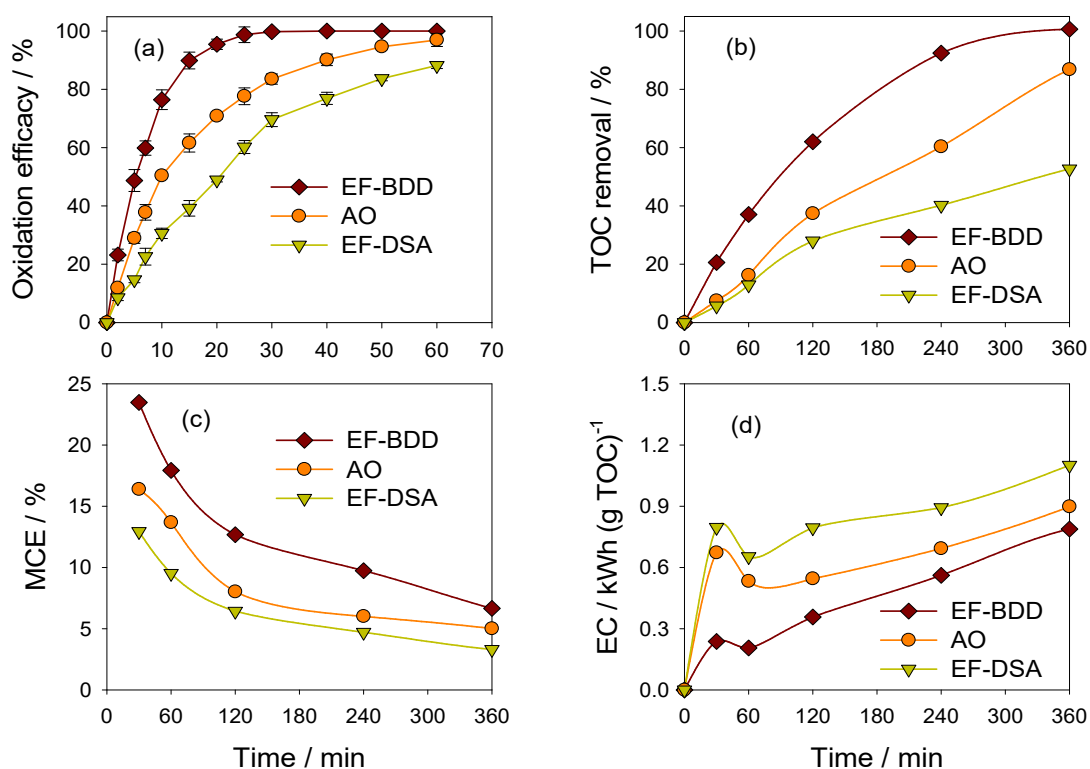
194 concentrations. Besides, Fe^{2+} can also be regenerated through other chemical reactions in the
 195 solution with slower kinetics (Eqs. (12) and (13)).



199 **Fig. 1:** Effect of concentration of catalyst Fe^{2+} on oxidation of OFLO by EF-BDD process and
 200 corresponding apparent rate constants. Conditions: Current density: 8.33 mA cm^{-2} , $[\text{Na}_2\text{SO}_4]$:
 201 50 mM, pH: 3.
 202
 203

204 The comparative oxidation efficiencies of different systems are given in Fig. 2. The oxidative
 205 degradation efficiency of OFLO was 100%, 90% and 76% in EF-BDD, AO and EF-DSA
 206 systems under current density of 8.3 mA cm^{-2} , upon electrolysis time of 40 min, respectively
 207 (Fig. 2(a)). In the EF-BDD process, OFLO could be completely disappeared at 30 min of
 208 electrolysis due to large amounts of BDD($\cdot\text{OH}$) generated on surface of anode (Eq. (1)) and
 209 homogeneous $\cdot\text{OH}$ generated in solution (Eq. (7)). The solution TOC was also completely
 210 removed upon electrolysis time of 6 h, which was much higher than that in the EF-DSA (53%)
 211 (Fig. 2(b)). The considerable performance of TOC removal in AO (87%) process was due to
 212 remarkable BDD($\cdot\text{OH}$) generated on surface of BDD anode. The mineralization current

213 efficiency (MCE) values (Eq. (4)) increased to peak values at early stages (1 h) of electrolysis
 214 in three systems (Fig. 2(c)), which can be attributed to quick degradation/mineralization of
 215 OFLO and intermediates by $\cdot\text{OH}$. Afterwards, the MCE decreased gradually with formation of
 216 recalcitrant by-products hardly oxidizable such as short chain carboxylic acids in solution and
 217 decrease in organic matter concentration. The values of energy consumption (Eq. (5)) for
 218 removal of TOC increased with treatment time and reached to 0.8, 0.9 and 1.1 kWh (g TOC)⁻¹
 219 in EF-BDD, AO and EF-DSA systems under 8.3 mA cm⁻², respectively (Fig. 2(d)). These
 220 results point out that EF-BDD is an outstanding process for oxidative degradation and
 221 mineralization of organic pollutants thanks to simultaneous production homogeneous $\cdot\text{OH}$ and
 222 heterogeneous BDD($\cdot\text{OH}$).

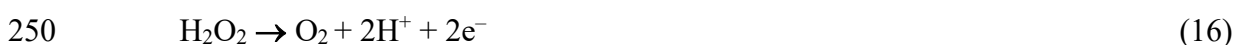


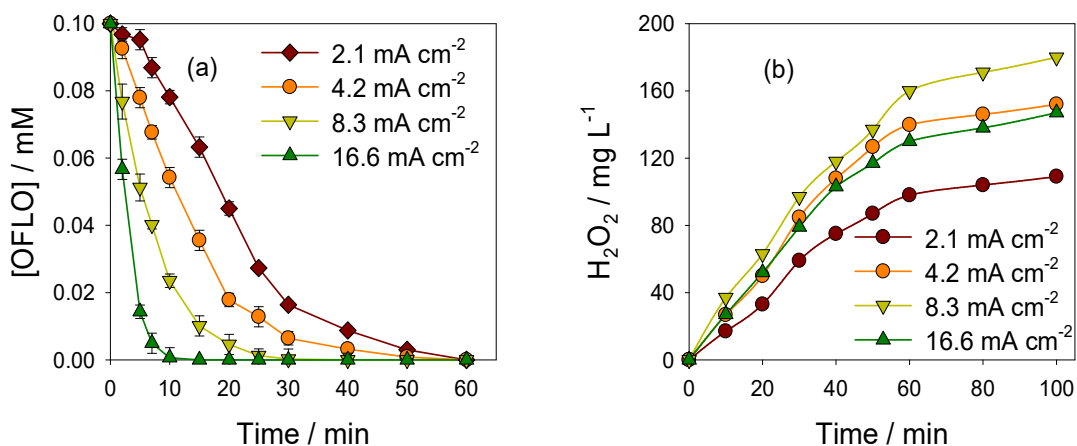
223
 224 **Fig. 2:** (a) Oxidation of OFLO; (b) TOC removal efficiency; (c) Mineralization current efficiency
 225 and (d) Energy consumption in EF-BDD, AO and EF-DSA systems. Conditions: Current
 226 density: 8.3 mA cm⁻², [Fe²⁺]: 0.2 mM, [Na₂SO₄]: 50 mM, pH: 3.

227

228 3.2. Effect of current densities on electrocatalytic activity of EF-BDD process

229 The formation of homogeneous $\cdot\text{OH}$ in solution and heterogeneous BDD($\cdot\text{OH}$) on the surface
230 of BDD anode are strongly related to applied current which monitor the formation of hydroxyl
231 radicals through Eqs. (1), (7) and (8) [4,34]. The effect of current on degradation kinetics of
232 OFLO is shown in Fig. (3). The complete oxidative degradation of 0.1 mM OFLO requires 60,
233 50, 30 and 10 min electrolysis time for 2.1, 4.2, 8.3 and 16.6 mA cm⁻² current densities (Fig.
234 3(a)). These results are in agreement with Fig. (1), highlighting the increase in k_{app} values of
235 OFLO oxidative degradation along with higher current densities (Fig. 4). When the current
236 density increased to 16.6 mA cm⁻², the k_{app} value (0.46 min⁻¹) of OFLO oxidation was more
237 than three times that at 8.3 mA cm⁻² (0.15 min⁻¹). High current densities have the advantage of
238 generating BDD($\cdot\text{OH}$), while being detrimental to production of H₂O₂ on cathode due to side
239 reactions. The generation of H₂O₂ increased with current densities from 2.1 to 8.3 mA cm⁻²,
240 while further increased current density (from 8.3 to 16.6 mA cm⁻²) led to a drop of H₂O₂
241 accumulation ((Fig. 3(b)). The generation of H₂O₂ reached to 180 mg L⁻¹ under 8.3 mA cm⁻²,
242 upon electrolysis time of 100 min, except for those have been activated by $\cdot\text{OH}$. The average
243 rates of H₂O₂ accumulation were 4.1, 5.8, 6.7 and 5.4 mg h⁻¹ cm⁻² under current densities of
244 2.1, 4.2, 8.3 and 16.6 mA cm⁻², respectively. It can be expected that the accumulation of H₂O₂
245 would suffer a predominant reduction when the current densities were higher than 16.6 mA
246 cm⁻². This can be explained with the competing reactions occurred at high current densities
247 [35,36].





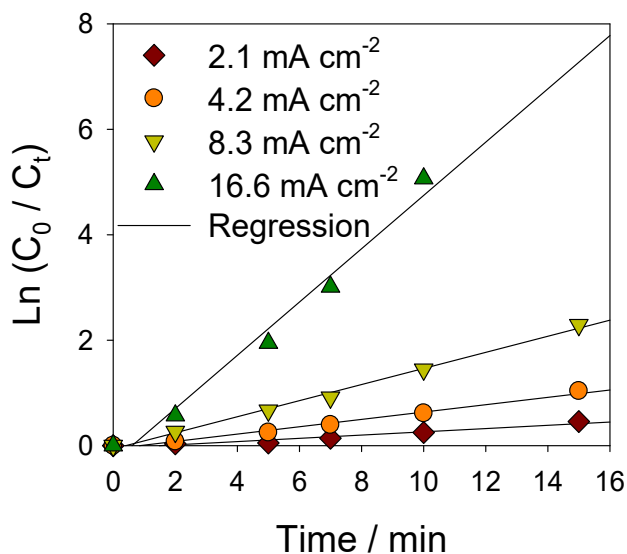
251

252 **Fig. 3** Effect of current densities on: (a) Decay kinetics of OFLO in EF-BDD process and (b)

253

Yield of H₂O₂ generation on the cathode.

254



255

256 **Fig. 4** Effect of current densities on the apparent rate constants for oxidation of OFLO.

257

Operating conditions: [Fe²⁺]: 0.2 mM, [Na₂SO₄]: 50 mM, pH: 3.

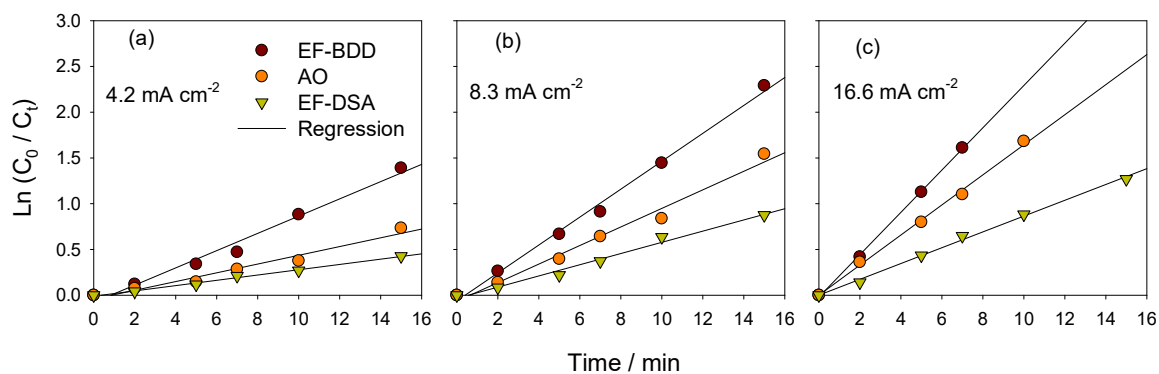
258

259 3.3. Synergistic effects of [•]OH and BDD([•]OH) on oxidation of OFLO

260 Effect of current densities on the apparent rate constants for oxidative removal of OFLO in EF-

261 BDD, AO and EF-DSA processes are presented in Fig. 5. The *k_{app}* values in EF-BDD (0.23

262 min^{-1}), AO (0.16 min^{-1}) and EF-DSA (0.09 min^{-1}) processes were greatest under 16.6 mA cm^{-2}
 263 2 , which were much higher than those obtained under 4.2 (0.09 , 0.04 and 0.03 min^{-1}) and 8.3
 264 (0.15 , 0.08 and 0.05 min^{-1}) mA cm^{-2} , respectively) (Fig. 6). The values of the synergistic factor
 265 (SF) were determined for oxidation of OFLO under different current densities.



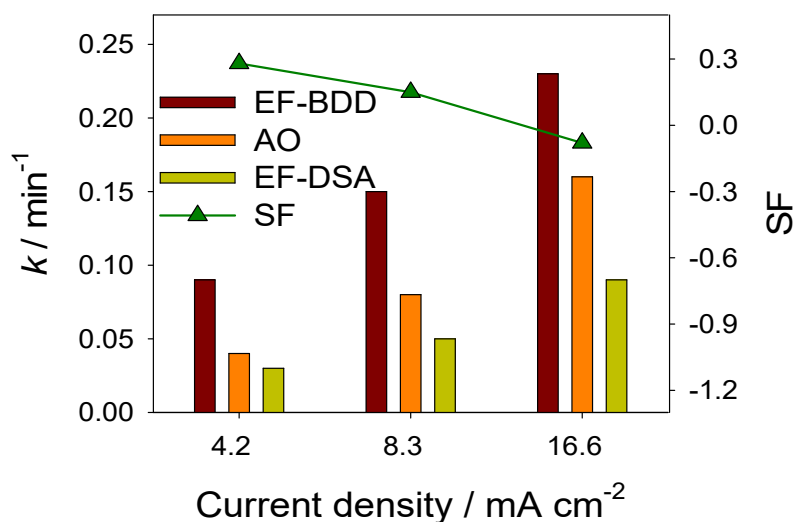
266
 267 **Fig. 5** Effect of current densities on the apparent rate constants for oxidative removal of
 268 OFLO in EF-BDD, AO and EF-DSA processes. Operating conditions: $[\text{Fe}^{2+}]$: 0.2 mM , $[\text{Na}_2\text{SO}_4]$:
 269 50 mM , pH : 3 .

270 Interestingly, the value of SF was 0.28 under current density of 4.2 mA cm^{-2} , and gradually
 271 decreased to 0.15 (8.3 mA cm^{-2}) and -0.08 (16.6 mA cm^{-2}), respectively. The results
 272 demonstrate the synergistic effects between homogeneous $\cdot\text{OH}$ and heterogeneous BDD($\cdot\text{OH}$)
 273 in EF-BDD under 4.2 and 8.3 mA cm^{-2} . The simultaneous generation of H_2O_2 on cathode and
 274 BDD($\cdot\text{OH}$) on the surface of anode contribute to the enhanced removal efficiencies of OFLO
 275 [25]. The SF value less than zero demonstrates no synergistic effects exist between $\cdot\text{OH}$ and
 276 BDD($\cdot\text{OH}$) in EF-BDD under 16.6 mA cm^{-2} . This can be explained by the fact that the rates of
 277 decay kinetics of OFLO in EF-BDD and AO were more convergent under 16.6 mA cm^{-2} with
 278 great amount of BDD($\cdot\text{OH}$) generated and dominated the degradation process.

279 As can be seen in Fig. 7, TOC removal efficiency is high during early stage of electrolysis (in
 280 first 2 h), afterwards, it becomes slower due to the diminution of organic matter in the solution
 281 and formation of refractory products, such as short-chain carboxylic acids [37-39]. The TOC
 282 removal efficiencies were 100% , 92.4% and 69% under 16.6 , 8.3 and 4.2 mA cm^{-2} in EF-BDD

283 processes, upon mineralization time of 240 min. These results were much higher than those
 284 obtained in AO (92%, 60.3% and 45%) and EF-DSA (61%, 40.2% and 26%) processes (Fig.
 285 7(a)-7(c)). The performance of TOC removal in EF-BDD process under 4.2 mA cm^{-2} was better
 286 than in AO process under 8.3 mA cm^{-2} , demonstrating the cost effectiveness of the EF process
 287 for mineralization of OFLO under low current densities [25]. This advantage is due to the
 288 simultaneous formation of homogeneous ($\cdot\text{OH}$) and heterogeneous (BDD($\cdot\text{OH}$)) hydroxyl
 289 radicals in the EF process.

290



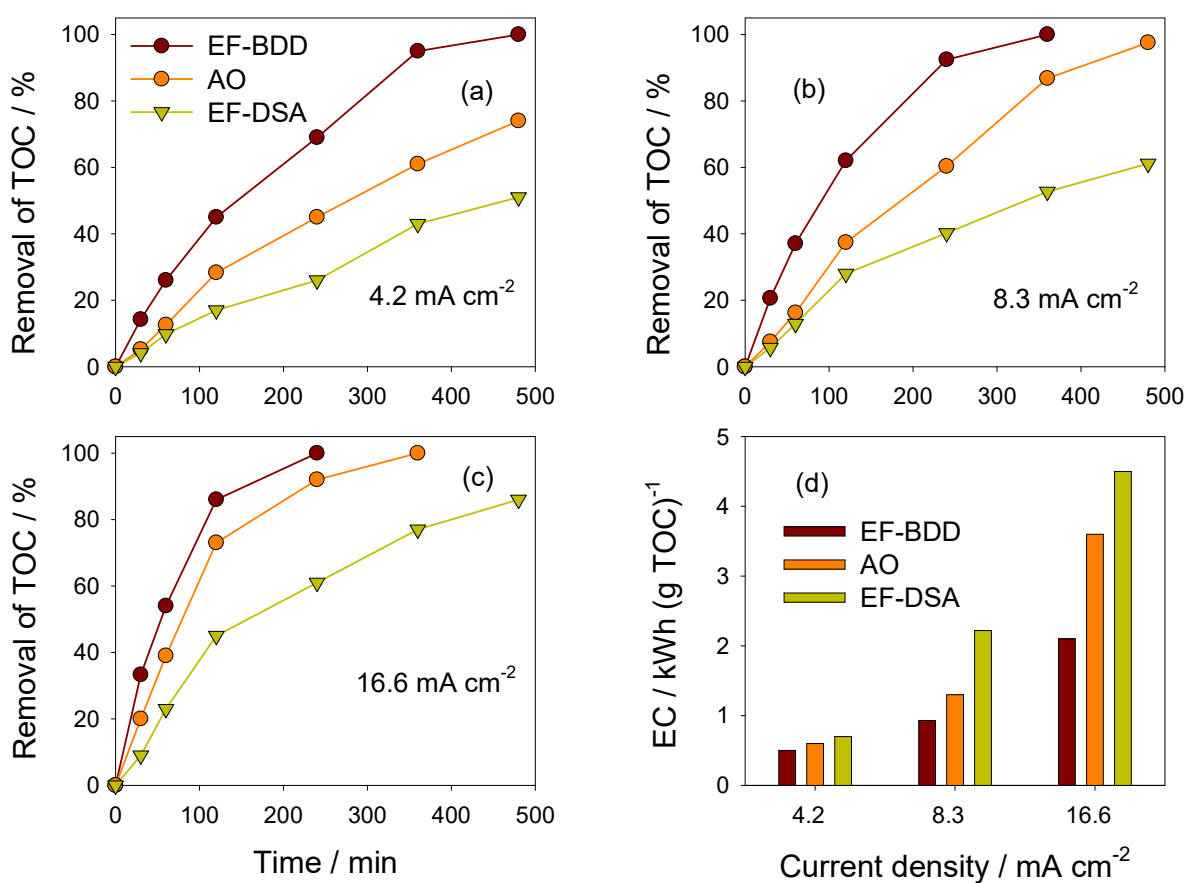
291

292 **Fig. 6** Synergistic factor (SF) of $\cdot\text{OH}$ and BDD($\cdot\text{OH}$) in EF-BDD and pseudo-first-order rate
 293 constant for OFLO removal under 4.2, 8.3 and 16.6 mA cm^{-2} . Conditions: $[\text{Fe}^{2+}]$: 0.2 mM (EF-
 294 BDD and EF-DSA), $[\text{Na}_2\text{SO}_4]$: 50 mM, pH: 3.

295

296 The values of EC increased with the rising current densities. Under current density of 4.2 mA
 297 cm^{-2} , the value of EC in AO ($0.6 \text{ kWh (gTOC)}^{-1}$), EF-DSA ($0.7 \text{ kWh (gTOC)}^{-1}$) and EF-BDD
 298 ($0.5 \text{ kWh (gTOC)}^{-1}$) processes was almost similar (Fig. 7(d)). In contrast, the value of EC in
 299 EF-DSA ($4.5 \text{ kWh (gTOC)}^{-1}$) was more than two times in EF-BDD (2.1 kWh m^{-3}) under 16.6
 300 mA cm^{-2} , demonstrating the cost effectiveness of BDD anodes for organics removal under high

301 current densities. It seems that the contribution of homogeneous $\cdot\text{OH}$ is not significant at high
 302 current densities since oxidation efficiencies in two processes presented few differences at 16.6
 303 mA cm^{-2} (Fig. 7(c)). However, the value of EC in AO (1.3 and 3.6 kWh (gTOC)^{-1}) was much
 304 higher than in EF-BDD (0.93 and 2.1 kWh (gTOC)^{-1}) under 8.3 and 16.6 mA cm^{-2} . Energy
 305 consumption for OFLO removal from wastewater could be reduced by 28%–41% in EF-BDD
 306 compared to AO process. Therefore, a balance need to be found between removal efficiencies
 307 and cost of disposal with BDD anode.



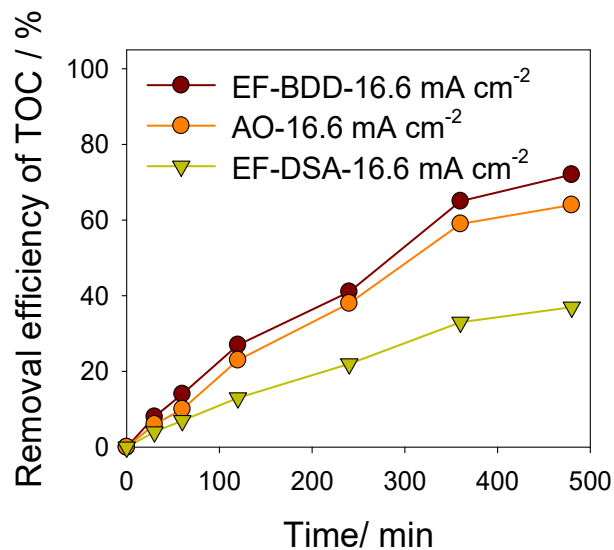
308
 309 **Fig. 7** (a-c) Removal efficiency of TOC and (d) values of EC for OFLO removal in EF-BDD, AO
 310 and EF-DSA processes under 4.2, 8.3 and 16.6 mA cm^{-2} . Conditions: $[\text{Fe}^{2+}]$: 0.2 mM (EF-BDD
 311 and EF-DSA, $[\text{Na}_2\text{SO}_4]$: 50 mM, pH: 3.
 312

313 To test the efficacy of the processes under examinations for the treatment of real wastewater,
 314 mineralization of a second wastewater effluent (SWE) collected from Guangzhou Liede
 315 sewage treatment plant (Table 1), was examined (Fig. 8). The TOC removal efficiencies were
 316 72%, 64% and 37% for EF-BDD, AO and EF-DSA processes under 16.6 mA cm^{-2} ,
 317 respectively, upon 480-min treatment time. Compared with the outstanding mineralization
 318 performance of synthetic OFLO solution (Fig. 7c), TOC removal efficiency was diminished
 319 for treatment of SWE. The decrease in mineralization efficiency during the treatment of SWE
 320 can be explained by (i) the presence of natural organic matter in SWE which could scavenge
 321 hydroxyl radicals that reduce the amount of $\cdot\text{OH}$ available for oxidation of OFLO and (ii)
 322 consumption of $\cdot\text{OH}$ in reactions with inorganic ions such as Cl^- and HCO_3^- present in SWE,
 323 with generation of less reactive radicals such as ClOH^- and $\text{CO}_3^{\cdot-}$ [23], [40].

324 **Table 1.** Quality parameters of secondary wastewater effluent.

pH	COD	TOC	Cl^-	HCO_3^-	CO_3^{2-}	Na^+
6.4	158 mg L^{-1}	10.2 mg L^{-1}	227 mg L^{-1}	129 mg L^{-1}	2.3 mg L^{-1}	28.5 mg L^{-1}

325

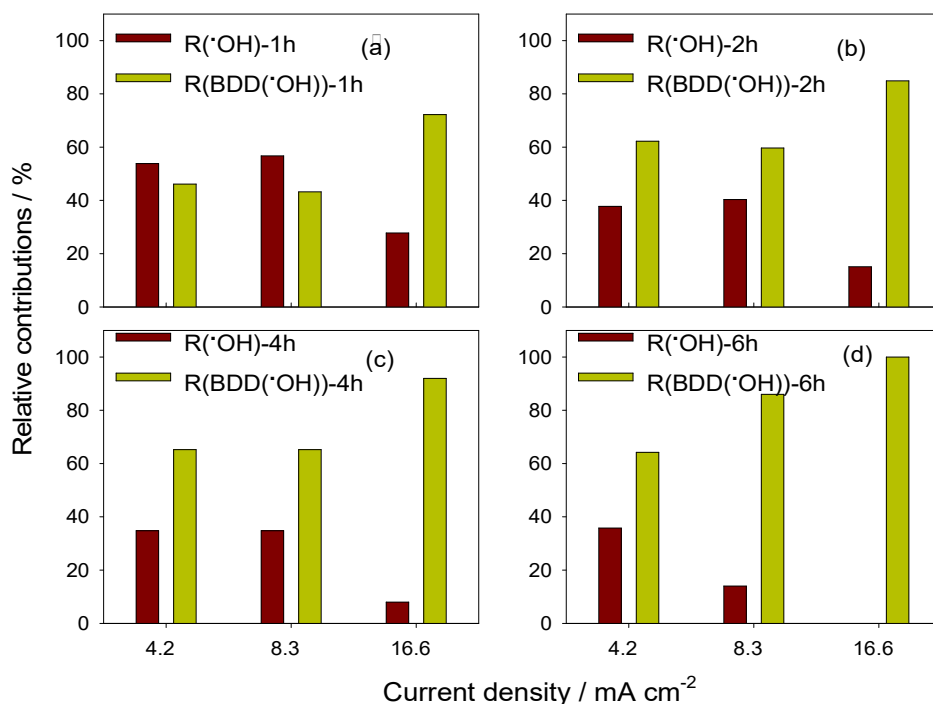


326

327 **Fig. 8** Removal efficiencies of TOC in SWE with EF-BDD, AO and EF-DSA processes under 16.6
 328 mA cm⁻². Operating conditions: [Fe²⁺]: 0.2 mM, [Na₂SO₄]: 50 mM, pH: 3.

329

330 The relative contribution of homogeneous [•]OH under 4.2 (54%) and 8.3 (57%) mA cm⁻² was
 331 higher than BDD([•]OH) upon electrocatalysis time of 1 h (Fig. 9). Subsequently, the
 332 contribution of [•]OH to the mineralization gradually slowed down and mineralization rate of
 333 OFLO is dominated by BDD([•]OH) after electrocatalysis time of 4 h. This result can be
 334 explained by two reasons: (i) formation of a large amount of BDD([•]OH) on the BDD anode,
 335 especially under high current densities and (ii) acceleration of electrons transfer rate leading to
 336 the mineralization of carboxylic acids [41], which are resistant to oxidation by [•]OH. When the
 337 current density increased to 16.6 mA cm⁻², the relative contributions of BDD([•]OH) reached to
 338 72%, 85%, 92% and 100% upon electrocatalysis time of 1, 2, 4 and 6 h, respectively. These
 339 results proved again that high current densities are advantageous to BDD([•]OH) production in
 340 EF-BDD process. These results were consistent to the similar TOC removal efficiencies in EF-
 341 BDD and AO processes under 16.6 mA cm⁻² (Fig. 7), where the mineralization of OFLO was
 342 dominated by BDD([•]OH).



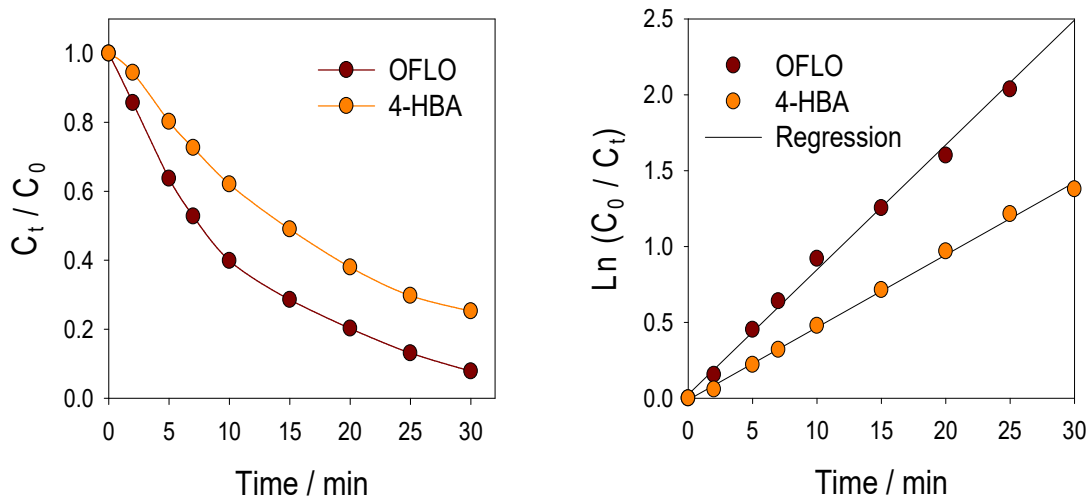
343

344 **Fig. 9** Relative contributions of homogeneous •OH and heterogeneous BDD(•OH) under 4.2,
 345 8.3 and 16.6 mA cm⁻² upon electrolysis time of (a) 1 h, (b) 2 h, (c) 4 h and (d) 6 h in EF-BDD
 346 processes. Operating conditions: [Fe²⁺]: 0.2 mM, [Na₂SO₄]: 50 mM, pH: 3.

347

348 *3.4. Determination of absolute rate constant of oxidation of OFLO by •OH*

349 The absolute (second order) rate constant of oxidation of OFLO by •OH (k_{OFLO}) was determined
 350 by competition kinetic method which is based on the competition for •OH between a substrate
 351 and a standard competitor for which the rate constant for its oxidation by •OH is known. Here,
 352 para-hydroxybenzoic acid (4-HBA) is taken as standard competitor because the rate constant
 353 of its oxidation by •OH is well-known as $2.19 \times 10^9 \text{ M}^{-1}\text{s}^{-1}$.



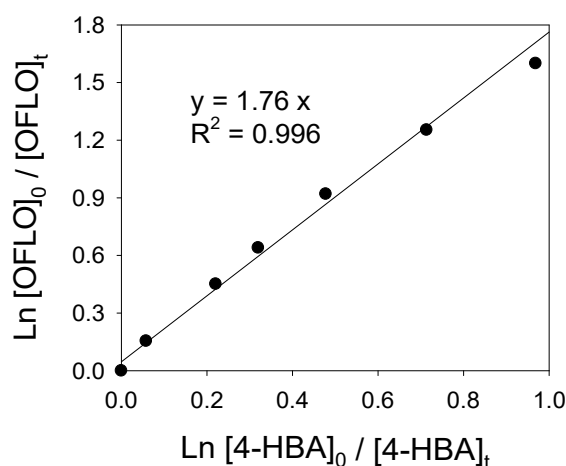
354
 355 **Fig. 10** (a) Decay kinetics and (b) Apparent rate constants of OFLO and 4-HBA in EF-BDD
 356 under current density of 2.1 mA cm⁻². Conditions: [Fe²⁺]: 0.2 mM, [Na₂SO₄]: 50 mM, pH: 3.
 357

358 The second order rate constant for oxidation of OFLO by [•]OH is then determined using Eq.
 359 (17) [12,42].

$$360 \quad \ln \left(\frac{[\text{OFLO}]_0}{[\text{OFLO}]_t} \right) = \frac{k_{\text{OFLO}}}{k_{4\text{-HBA}}} \times \ln \left(\frac{[4\text{-HBA}]_0}{[4\text{-HBA}]_t} \right) \quad (17)$$

361 The rate constant for OFLO oxidation by OH can be determined from the slope of the linear
 362 plot of $\ln ([\text{OFLO}]_0/[\text{OFLO}]_t) = f(\ln ([4\text{-HBA}]_0/[4\text{-HBA}]_t))$.

363 Electrolysis were carried out under low current (2.1 mA cm⁻²) and short time (30 min) to avoid
 364 the interference of the intermediate formed, using same concentration (0.1 mM) of OFLO and
 365 4-HBA. Competitive degradation kinetics and determination of k_{OFLO} are presented in Figs. 10
 366 and 11. The apparent rate constant for oxidative degradation of OFLO with [•]OH (0.08 min⁻¹)
 367 was two-fold of the one between 4-HBA and [•]OH (0.04 min⁻¹) and k_{OFLO} was calculated to be
 368 $3.86 \times 10^9 \text{ M}^{-1}\text{s}^{-1}$ (Fig. 11).



369

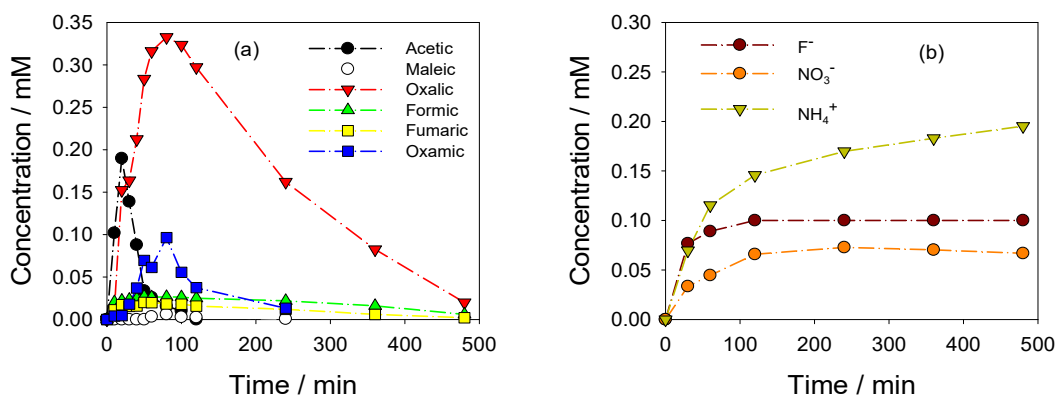
370 **Fig. 11** Determination of the absolute (second order) rate constant of oxidation of OFLO by
 371 $\cdot\text{OH}$ (k_{OFLO}) using 4-HBA as standard competitor under current of 2.1 mA cm^{-2} .

372

373 *3.5. Formation and evolution of short-chain carboxylic acids and inorganic ions in EF-*
 374 *BDD process*

375 During the mineralization of 0.1 mM OFLO solution by EF-BDD process, six short-chain
 376 carboxylic acids were identified and followed upon electrolysis time of 8 h (Fig. 12(a)). Acetic,
 377 formic, oxamic and oxalic acids appeared at retention time of 9.2, 12.9, 14.2, and 15.7 min,
 378 respectively, during their analysis by ion-exclusion chromatography. Maleic and fumaric acids
 379 were detected in trace level. The concentration of carboxylic acids quickly reached peak values
 380 at the early stage of electrocatalysis time (120 min) and gradually decreased with further
 381 electrolysis time. Oxalic acid attained the highest concentration (0.33 mM) after 1 h of
 382 electrolysis. Oxalic and oxamic acids, which are resistant to the attack by $\cdot\text{OH}$ radicals [25],
 383 reached 0.16 and 0.01 mM upon electrocatalysis time of 4 h. After electrocatalysis time of 4 h,
 384 heterogeneous BDD($\cdot\text{OH}$) dominated the mineralization of short-chain organic acids (ultimate
 385 by-products) before mineralization to CO_2 and H_2O via direct electro-transfer oxidation
 386 reactions on the surface of BDD anode since the rate constant of carboxylic acids with

387 homogeneous $\cdot\text{OH}$ is pretty low [25]. These results are in agreement with the TOC decay values
388 obtained in EF-BDD process (Fig. 7) and relative contributions of BDD($\cdot\text{OH}$) in Fig. 9.



389
390 **Fig. 12** Time-course of identified carboxylic acids (a) and inorganic ions (b) generated during
391 mineralization of 0.10 mM OFLO solution by EF-BDD process. Conditions: $[\text{Fe}^{2+}]$: 0.2 mM,
392 current density: 16.6 mA cm^{-2} , $[\text{Na}_2\text{SO}_4]$: 50 mM, pH: 3.

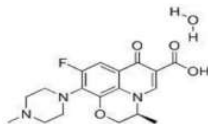
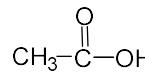
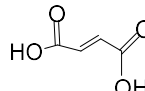
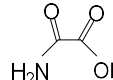
393
394 The target pollutant OFLO molecule contains N and F atoms, which can be released into
395 solution as NH_4^+ , NO_2^- , NO_3^- and F^- . The concentrations of NH_4^+ and NO_3^- increased with
396 electrocatalysis time and gradually reached to plateaus, with cumulative concentration of 0.2
397 mM NH_4^+ and 0.07 mM NO_3^- (Fig. 12(b)). The continuous increase in NH_4^+ concentration is
398 due to cathodic reduction of formed NO_3^- to NH_4^+ [19]. NO_2^- was not detected in this study
399 since no NO_2^- generated during the mineralization process or the concentration of accumulated
400 NO_2^- formed is under the detection limit. About 90% of the nitrogen initially present in OFLO
401 solution (0.3 mM) is detected as NH_4^+ and NO_3^- , and 10% lost in N can be explained by the
402 probable formation of gaseous nitrogen compounds (N_2 , NO_x , N_2O_5) [43]. As well, the
403 concentration of accumulated F^- increased rapidly during electrolysis time of 120 min,
404 afterwards kept constant with little fluctuation. The mass balance for F is quasi-complete since
405 the amount of F present in initial OFLO molecule (0.1 mM) was released as F^- into the treated
406 solution.

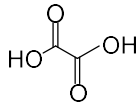
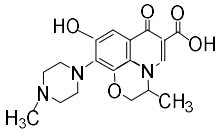
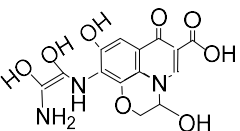
407

408 3.6. Toxicity assessment of OFLO and intermediates in EF-BDD process

409 Generally, some intermediates formed during AOPs treatment would be more toxic than the
 410 initial organic pollutants, leading to types of environmental problems [44,45]. The
 411 transformation products (OTPs) identified during oxidation of OFLO, using HPLC and GC-
 412 MS analyses were presented in Table 2. Two cyclic compounds (OTP5 and OTP6) were
 413 detected in addition of four main short chain carboxylic acids. In EF-BDD process,
 414 defluorination reaction occurred at the first stage of electrooxidation as shown in Fig. 12b.
 415 Meanwhile, piperazinyl ring was attacked by $\cdot\text{OH}/\text{BDD}(\cdot\text{OH})$ causing dealkylation. Short-
 416 chain carboxylic acids generated through progressive oxidative cleavage of aromatic rings and
 417 further oxidation of aliphatics structures. Values of LC_{50} , developmental toxicity and
 418 bioaccumulation factor of OTPs were calculated by quantitative structure activity relationship
 419 predication using Toxicity Estimation Software Tool (T.E.S.T.) software [46]. Acute toxicity
 420 expressed in LC_{50} value of OTP1, OTP2, OTP3 and OTP4 was 60.8, 11.8, 18.1 and 85 times
 421 that of OFLO (17 mg L^{-1}), respectively, and these OTPs were considered as “not harmful” (Fig.
 422 13(a)). The developmental toxicity of OFLO (1.03) was higher than that of OTP1,

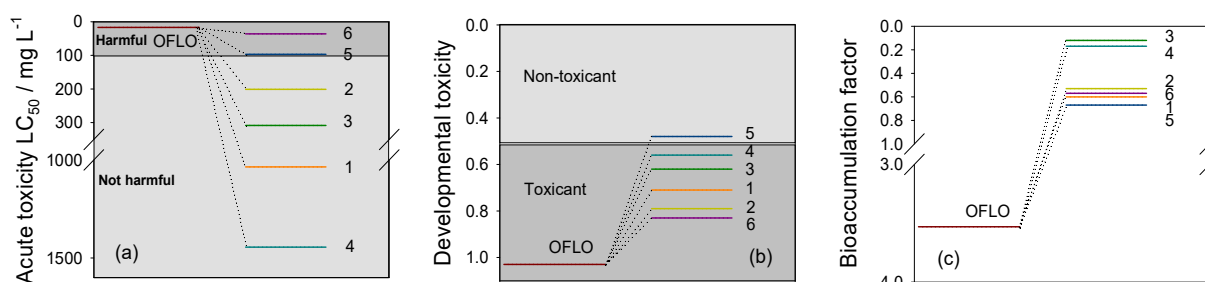
423 **Table 2.** OFLO transformation products (OTPs) generated in EF-BDD process.

Compound	Molecular mass (g mol^{-1})	Molecular structure	Retention time (min)
OFLO	361.1		27.2
OTP 1 (Acetic)	60		9.2
OTP 2 (Fumaric)	116		14.2
OTP 3 (Oxamic)	89		15.5

OTP 4 (Oxalic)	90		15.7
OTP 5	360		22
OTP 6	326		25

424

425 OTP2, OTP3 and OTP6 was considered “developmental toxicant” (Fig. 13(b)). Values of
 426 developmental toxicity proved that OTP4 and OTP5 were “developmental non-toxicant”. The
 427 bioaccumulation factor of OTPs (OTP1 (0.6), OTP2 (0.53), OTP3 (0.12), OTP4 (0.17), OTP5
 428 (0.67) and OTP6 (0.57) decreased more than 80% compared with that of OFLO (3.53) (Fig.
 429 13(c)). In short, the toxicity of OTPs was assessed as much lower than that of OFLO.



430

431 **Fig. 13** Determination of acute toxicity (a); developmental toxicity (b) and bioaccumulation
 432 factor (c) of OFLO and OFLO transformation products (OTPs). Numbers 1 to 6 represent
 433 OTP1 to OTP6, respectively.

434 4. Conclusions

435 The present study explored the reactivity and mechanism of EF-BDD process for removal of
 436 the antibiotic ofloxacin from water. High current densities were found to be beneficial to
 437 generation of BDD(*OH) because of more converging decay kinetics rates of OFLO in EF-
 438 BDD and AO processes. EF-BDD process was more efficient in removing solution TOC
 439 compared to AO process due to the simultaneous formation of homogeneous (*OH) and

440 heterogeneous (BDD(\cdot OH)) hydroxyl radicals in the former one. For example, TOC removal
441 efficiency of EF-BDD process under 4.2 mA cm^{-2} was better than that of AO process under 8.3
442 mA cm^{-2} . In EF-BDD process, the synergistic factor of \cdot OH and BDD(\cdot OH) decreased with
443 current density rising from $4.2 (0.28)$ to $16.6 (-0.08) \text{ mA cm}^{-2}$. The value of EC in EF-DSA
444 ($4.5 \text{ kWh (gTOC)}^{-1}$) was more than two times of that in EF-BDD (2.1 kWh m^{-3}) under 16.6
445 mA cm^{-2} . Evolution of carboxylic acids, inorganic ions (NH_4^+ , NO_3^- and F^-) and toxicity
446 assessment in treated solution prove the complete mineralization of OFLO in EF-BDD process.
447 This study show that EF-BDD process could provide great potential to treatment of antibiotics
448 wastewater, and a balance need to be found between removal efficiencies and energy
449 consumption with BDD anode.

450

451 **CRedit authorship contribution statement**

452 **Weilu Yang:** Conceptualization, Methodology, Investigation, Writing original draft, Funding
453 acquisition. **Nihal Oturan, Mehmet A Oturan:** Writing – review & editing, Funding
454 acquisition.

455

456 **Declaration of Competing Interest**

457 The authors declare no competing financial interest.

458

459 **Acknowledgements**

460 The present study was financially supported by National Natural Science Foundation of China
461 (Nos. 22006053) and Guangdong Basic and Applied Basic Research Foundation
462 (2019A1515110797).

463

References

- [1] E. Hapeshi, A. Achilleos, M.I. Vasquez, C. Michael, N.P. Xekoukoulotakis, D. Mantzavinos, D. Kassinos, Drugs degrading photocatalytically: kinetics and mechanisms of ofloxacin and atenolol removal on titania suspensions, *Water research*, 44 (2010) 1737-1746. [10.1016/j.watres.2009.11.044](https://doi.org/10.1016/j.watres.2009.11.044)
- [2] A. Dirany, S. Efremova Aaron, N. Oturan, I. Sirés, M.A. Oturan, J. Aaron, Study of the toxicity of sulfamethoxazole and its degradation products in water by a bioluminescence method during application of the electro-Fenton treatment, *Analytical and bioanalytical chemistry*, 400 (2011) 353-360. <https://doi.org/10.1007/s00216-010-4441-x>
- [3] A. Jurado, M. Walther, M.S. Díaz-Cruz, Occurrence, fate and environmental risk assessment of the organic microcontaminants included in the Watch Lists set by EU Decisions 2015/495 and 2018/840 in the groundwater of Spain, *Science of the Total Environment*, 663 (2019) 285-296. <https://doi.org/10.1016/j.scitotenv.2019.01.270>
- [4] I. Sirés, E. Brillas, M.A. Oturan, M.A. Rodrigo, M. Panizza, Electrochemical advanced oxidation processes: today and tomorrow. A review, *Environmental Science and Pollution Research*, 21 (2014) 8336-8367. <https://doi.org/10.1007/s11356-014-2783-1>
- [5] E. Brillas, I. Sirés, M.A. Oturan, Electro-Fenton process and related electrochemical technologies based on Fenton's reaction chemistry, *Chemical reviews*, 109 (2009) 6570-6631. <https://doi.org/10.1021/cr900136g>
- [6] X.D. Du, M.A. Oturan, M.H. Zhou, N. Belkessa, P. Su, J.J. Cai, C. Trelu, E. Mousset, Nanostructured electrodes for electrocatalytic advanced oxidation processes: From materials preparation to mechanisms understanding and wastewater treatment applications, *Applied Catalysis B: Environmental*, 296 (2021), 120332. <https://doi.org/10.1016/j.apcatb.2021.120332>
- [7] P. V. Nidheesh, S. O. Ganiyu, C. A. Martínez-Huitle, E. Mousset, H. Olvera-Vargas, Trelu, C. Trelu, M.H. Zhou, Oturan, M. A, Recent advances in electro-Fenton process and its emerging applications. *Critical Reviews in Environmental Science and Technology*, (2022) 1-27. <https://doi.org/10.1080/10643389.2022.2093074>
- [8] H. Zhao, Y. Chen, Q. Peng, Q. Wang, G. Zhao, Catalytic activity of MOF (2Fe/Co)/carbon aerogel for improving H₂O₂ and OH generation in solar photo-electro-Fenton process, *Applied Catalysis B: Environmental*, 203 (2017) 127-137. <https://doi.org/10.1016/j.apcatb.2016.09.074>
- [9] H. Zhao, L. Qian, X. Guan, D. Wu, G. Zhao, Continuous bulk FeCuC aerogel with ultradispersed metal nanoparticles: an efficient 3D heterogeneous electro-Fenton cathode over a wide range of pH 3–9, *Environmental Science & Technology*, 50 (2016) 5225-5233. <https://doi.org/10.1021/acs.est.6b00265>
- [10] H. Olvera-Vargas, J. Dubuc, Z. Wang, L. Coudert, C.M. Neculita, O. Lefebvre, Electro-Fenton beyond the degradation of organics: Treatment of thiosalts in contaminated mine water, *Environmental Science & Technology*, 55 (2021) 2564-2574. <https://doi.org/10.1021/acs.est.0c06006>
- [11] S. Cheng, H. Zheng, C. Shen, B. Jiang, F. Liu, A. Li, Hierarchical iron phosphides composite confined in ultrathin carbon layer as effective heterogeneous electro-Fenton catalyst with prominent stability and catalytic activity, *Advanced Functional Materials*, 31 (2021) 2106311. <https://doi.org/10.1002/adfm.202106311>

- [12] S. Camcioglu, B. Özyurt, N. Oturan, C. Trellu, M.A. Oturan, Fast and complete destruction of the anti-cancer drug Cytarabine from water by electrocatalytic oxidation using electro-Fenton process. *Catalysts*, 12 (2022) 1598. <https://doi.org/10.3390/catal12121598>
- [13] C. Trellu, M. Gibert-Vilas, Y. Péchaud, N. Oturan, M.A. Oturan, Clofibric acid removal at activated carbon fibers by adsorption and electro-Fenton regeneration – Modeling and limiting phenomena, *Electrochimica Acta*, 382 (2021) 138283. <https://doi.org/10.1016/j.electacta.2021.138283>
- [14] F. Sopaj, N. Oturan, J. Pinson, F. Podvorica, M.A. Oturan, Effect of the anode materials on the efficiency of the electro-Fenton process for the mineralization of the antibiotic sulfamethazine, *Applied Catalysis B: Environmental*, 199 (2016) 331-341. <https://doi.org/10.1016/j.apcatb.2016.06.035>
- [15] M. Zhao, Z. Cui, L. Fu, F. Ndayisenga, D. Zhou, Shewanella drive Fe (III) reduction to promote electro-Fenton reactions and enhance Fe inner-cycle, *ACS ES&T Water*, 1 (2020) 613-620. <https://doi.org/10.1021/acsestwater.0c00126>
- [16] M.H. Zhou, M.A. Oturan, I. Sirés, (Eds.), "Electro-Fenton Process: New trends and scale-up". *The handbook of environmental chemistry*, volume 61. Springer, Singapore, 2018, ISBN: ISBN: 978-981-10-6405-0
- [17] J. Ma, C. Trellu, N. Oturan, S. Raffy, M.A. Oturan, Development of Ti/TiO_x foams for removal of organic pollutants from water: Influence of porous structure of Ti substrate, *Applied Catalysis B: Environmental*, 317 (2022) 121736. <https://doi.org/10.1016/j.apcatb.2022.121736>
- [18] Z. Hu, J.J. Cai, G. Song, Y.S. Tian, M.H. Zhou, Anodic oxidation of organic pollutants: anode fabrication, process hybrid and environmental applications. *Current Opinion in Electrochemistry*, 26 (2021) 100659. <https://doi.org/10.1016/j.coelec.2020.100659>
- [19] W.L. Yang, N. Oturan, S. Raffy, M.H. Zhou, M.A. Oturan, Electrocatalytic generation of homogeneous and heterogeneous hydroxyl radicals for cold mineralization of anti-cancer drug Imatinib, *Chemical Engineering Journal*, 383 (2020) 123155. <https://doi.org/10.1016/j.cej.2019.123155>
- [20] Y. Chen, C.J. Miller, T.D. Waite, Heterogeneous Fenton chemistry revisited: Mechanistic insights from ferrihydrite-mediated oxidation of formate and oxalate, *Environmental Science & Technology*, 55 (2021) 14414-14425. <https://doi.org/10.1021/acs.est.1c00284>
- [21] Y. Zhu, R. Zhu, Y. Xi, J. Zhu, G. Zhu, H. He, Strategies for enhancing the heterogeneous Fenton catalytic reactivity: a review, *Applied Catalysis B: Environmental*, 255 (2019) 117739. <https://doi.org/10.1016/j.apcatb.2019.05.041>
- [22] H. Sheng, A.N. Janes, R.D. Ross, D. Kaiman, J. Huang, B. Song, J. Schmidt, S. Jin, Stable and selective electrosynthesis of hydrogen peroxide and the electro-Fenton process on CoSe₂ polymorph catalysts, *Energy & Environmental Science*, 13 (2020) 4189-4203. <https://doi.org/10.1039/D0EE01925A>
- [23] S.A. Hien, C. Trellu, N. Oturan, A.S. Assémian, B.G.H. Briton, P. Drogui, K. Adouby, M.A. Oturan, Comparison of homogeneous and heterogeneous electrochemical advanced oxidation processes for treatment of textile industry wastewater, *Journal of Hazardous Materials*, (2022) 129326. <https://doi.org/10.1016/j.jhazmat.2022.129326>

- [24] A. Özcan, Y. Şahin, A.S. Koparal, M.A. Oturan, Protham mineralization in aqueous medium by anodic oxidation using boron-doped diamond anode: influence of experimental parameters on degradation kinetics and mineralization efficiency, *Water research*, 42 (2008) 2889-2898. <https://doi.org/10.1016/j.watres.2008.02.027>
- [25] H. Olvera-Vargas, N. Gore-Datar, O. Garcia-Rodriguez, S. Mutnuri, O. Lefebvre, Electro-Fenton treatment of real pharmaceutical wastewater paired with a BDD anode: reaction mechanisms and respective contribution of homogeneous and heterogeneous OH, *Chemical Engineering Journal*, 404 (2021) 126524. <https://doi.org/10.1016/j.watres.2008.02.027>
- [26] M.A. Oturan, Outstanding performances of the BDD film anode in electro-Fenton process: Applications and comparative performance, *Current Opinion in Solid State and Materials Science*, 25 (2021) 100925. <https://doi.org/10.1016/j.cossms.2021.100925>
- [27] Q. Wang, M. Liu, H. Zhao, Y. Chen, F. Xiao, W. Chu, G. Zhao, Efficiently degradation of perfluorooctanoic acid in synergic electrochemical process combining cathodic electro-Fenton and anodic oxidation, *Chemical Engineering Journal*, 378 (2019) 122071. <https://doi.org/10.1016/j.cej.2019.122071>
- [28] H. Olvera - Vargas, V.Y.H. Wee, O. Garcia - Rodriguez, O. Lefebvre, Near - neutral Electro - Fenton Treatment of Pharmaceutical Pollutants: Effect of Using a Triphosphate Ligand and BDD Electrode, *ChemElectroChem*, 6 (2019) 937-946. <https://doi.org/10.1002/celec.201801732>
- [29] W. Yang, M. Zhou, J. Cai, L. Liang, G. Ren, L. Jiang, Ultrahigh yield of hydrogen peroxide on graphite felt cathode modified with electrochemically exfoliated graphene, *Journal of Materials Chemistry A*, 5 (2017) 8070-8080. <https://doi.org/10.1039/C7TA01534H>
- [30] W.L. Yang, M.H. Zhou, N. Oturan, Y.W. Li, M.A. Oturan, Electrocatalytic destruction of pharmaceutical imatinib by electro-Fenton process with graphene-based cathode, *Electrochimica Acta*, 305 (2019) 285-294. <https://doi.org/10.1016/j.electacta.2019.03.067>
- [31] O. Garcia-Rodriguez, Y.Y. Lee, H. Olvera-Vargas, F. Deng, Z. Wang, O. Lefebvre, Mineralization of electronic wastewater by electro-Fenton with an enhanced graphene-based gas diffusion cathode, *Electrochimica Acta*, 276 (2018) 12-20. <https://doi.org/10.1016/j.electacta.2018.04.076>
- [32] J. Casado, Towards industrial implementation of Electro-Fenton and derived technologies for wastewater treatment: A review, *Journal of Environmental Chemical Engineering*, 7 (2019) 102823. <https://doi.org/10.1016/j.jece.2018.102823>
- [33] N. Barhoumi, H. Olvera-Vargas, N. Oturan, D. Huguenot, A. Gadri, S. Ammar, E. Brillas, M.A. Oturan, Kinetics of oxidative degradation/mineralization pathways of the antibiotic tetracycline by the novel heterogeneous electro-Fenton process with solid catalyst chalcopyrite, *Applied Catalysis B: Environmental*, 209 (2017) 637-647. <https://doi.org/10.1016/j.apcatb.2017.03.034>
- [34] N. Oturan, J. Bo, C. Trelu, M.A. Oturan, Comparative performance of ten electrodes in electro - Fenton process for removal of organic pollutants from water, *ChemElectroChem*, 8 (2021) 3294-3303. <https://doi.org/10.1002/celec.202100588>
- [35] F.C. Moreira, R.A. Boaventura, E. Brillas, V.J. Vilar, Electrochemical advanced oxidation processes: a review on their application to synthetic and real wastewaters,

- Applied Catalysis B: Environmental, 202 (2017) 217-261.
<https://doi.org/10.1016/j.apcatb.2016.08.037>
- [36] F. Ghanbari, A. Hassani, S. Waclawek, Z. Wang, G. Matyszcak, K.Y.A. Lin, M. Dolatabadi, Insights into paracetamol degradation in aqueous solutions by ultrasound-assisted heterogeneous electro-Fenton process: Key operating parameters, mineralization and toxicity assessment, Separation and Purification Technology, 266 (2021) 118533.
<https://doi.org/10.1016/j.seppur.2021.118533>
- [37] W.L. Yang, M.H. Zhou, N. Oturan, Y.W. Li, P. Su, M.A. Oturan, Enhanced activation of hydrogen peroxide using nitrogen doped graphene for effective removal of herbicide 2, 4-D from water by iron-free electrochemical advanced oxidation, Electrochimica Acta, 297 (2019) 582-592. <https://doi.org/10.1016/j.electacta.2018.11.196>
- [38] S.O. Ganiyu, N. Oturan, S. Raffy, M. Cretin, R. Esmilaire, E.V. Hullebusch, G. Esposito, M.A. Oturan, Sub-stoichiometric titanium oxide (Ti₄O₇) as a suitable ceramic anode for electrooxidation of organic pollutants: a case study of kinetics, mineralization and toxicity assessment of amoxicillin. Water Research, 106 (2016) 171-182.
<https://doi.org/10.1016/j.watres.2016.09.056>
- [39] H. Lin, N. Oturan, J. Wu, V.K. Sharma, H. Zhang, M. A. Oturan, Removal of artificial sweetener aspartame from aqueous media by electrochemical advanced oxidation processes. Chemosphere, 167 (2017) 220-227.
<https://doi.org/10.1016/j.chemosphere.2016.09.143>
- [40] W.L. Yang, M.S. Zhu, W.B. Li, G.L. Liu, E.Y. Zeng, Surface-catalyzed electro-Fenton with flexible nanocatalyst for removal of plasticizers from secondary wastewater effluent, Journal of Hazardous Materials, 435 (2022) 129023.
- [41] S. Garcia-Segura, E. Brillas, Mineralization of the recalcitrant oxalic and oxamic acids by electrochemical advanced oxidation processes using a boron-doped diamond anode, Water research, 45 (2011) 2975-2984.
- [42] M. Mbaye, P.A. Diaw, O.M.A. Mbaye, N. Oturan, M.D. Gaye Seye, C. Trelu, A. Coly, A. Tine, J.J. Aaron, M.A. Oturan, Rapid removal of fungicide thiram in aqueous medium by electro-Fenton process with Pt and BDD anodes, Separation and Purification Technology, 281 (2022) 119837. <https://doi.org/10.1016/j.seppur.2021.119837>
- [43] S. Garcia-Segura, E. Mostafa, H. Baltruschat, Could NO_x be released during mineralization of pollutants containing nitrogen by hydroxyl radical? Ascertaining the release of N-volatile species, Applied Catalysis B: Environmental, 207 (2017) 376-384.
- [44] A. Dirany, I. Sires, N. Oturan, A. Özcan, M.A. Oturan, Electrochemical treatment of the antibiotic sulfachloropyridazine: kinetics, reaction pathways, and toxicity evolution, Environmental science & technology, 46 (2012) 4074-4082.
- [45] E. Brillas, B. Boye, I. Sirés, J.A. Garrido, R.M. Rodríguez, C. Arias, P.L. Cabot, C. Comninellis, Electrochemical destruction of chlorophenoxy herbicides by anodic oxidation and electro-Fenton using a boron-doped diamond electrode, Electrochimica Acta, 49 (2004) 4487-4496.
- [46] J.J. Jiang, X.Y. Wang, C.J. Zhang, T.R. Li, Y.L. Lin, T.F. Xie, S.S. Dong, Porous 0D/3D NiCo₂O₄/g-C₃N₄ accelerate emerging pollutant degradation in PMS/vis system: Degradation mechanism, pathway and toxicity assessment. Chemical Engineering Journal, 397 (2020) 125356. <https://doi.org/10.1016/j.cej.2020.125356>